NREL
NATIONAL RENEWABLE ENERGY LABORATORY

High-Temperature Phase Change Materials (PCM) Candidates for Thermal Energy Storage (TES) Applications

Judith C. Gomez

NREL is a national laboratory of the U.S. Department of Energy, Office of Energy Efficiency & Renewable Energy, operated by the Alliance for Sustainable Energy, LLC.

Milestone Report
NREL/TP-5500-51446
September 2011

Contract No. DE-AC36-08GO28308

NREL
NATIONAL RENEWABLE ENERGY LABORATORY

High-Temperature Phase Change Materials (PCM) Candidates for Thermal Energy Storage (TES) Applications

Judith C. Gomez

Prepared under Task No. CP09.2201

National Renewable Energy Laboratory
1617 Cole Boulevard
Golden, Colorado 80401
303-275-3000 • www.nrel.gov

Milestone Report
NREL/TP-5500-51446
September 2011

Contract No. DE-AC36-08GO28308

NOTICE

Available electronically at http://www.osti.gov/bridge

Available for a processing fee to U.S. Department of Energy and its contractors, in paper, from:

U.S. Department of Energy
Office of Scientific and Technical Information

P.O. Box 62
Oak Ridge, TN 37831-0062
phone: 865.576.8401
fax: 865.576.5728
email: mailto:reports@adonis.osti.gov

Available for sale to the public, in paper, from:

U.S. Department of Commerce
National Technical Information Service
5285 Port Royal Road
Springfield, VA 22161
phone: 800.553.6847
fax: 703.605.6900
email: orders@ntis.fedworld.gov
online ordering: http://www.ntis.gov/help/ordermethods.aspx

Cover Photos: (left to right) PIX 16416, PIX 17423, PIX 16560, PIX 17613, PIX 17436, PIX 17721

Printed on paper containing at least 50% wastepaper, including 10% post consumer waste.

Table of Contents

List of Tables

List of Figures

1 Introduction

It is clearly understood that lower overall costs are a key factor to make renewable energy technologies competitive with traditional energy sources. Energy storage technology is one path to increase the value and reduce the cost of all renewable energy supplies.

Concentrating solar power (CSP) technologies have the ability to dispatch electrical output to match peak demand periods by employing thermal energy storage (TES). In addition, TES can reduce the levelized cost of energy (LCOE) for CSP plants. In order to achieve this, energy storage technologies require efficient materials with high energy density.

To store thermal energy, sensible and latent heat storage materials are widely used. Latent heat TES systems using phase change material (PCM) are useful because of their ability to charge and discharge a large amount of heat from a small mass at constant temperature during a phase transformation like melting-solidification. PCM technology relies on the energy absorption/liberation of the latent heat during a physical transformation. Unlike vapor-liquid transformations, solid-liquid transformations produce large enthalpy changes without large density changes, and due to this, salts and metallic alloys are good candidates for PCMs. Ideally these materials should have a specific melting point and high heat of fusion, and offer favorable characteristics such as high working temperatures (over 500°C), low vapor pressure, good thermal and physical properties, low corrosivity and toxicity, and, of course, low cost.

Because high-melting-point PCMs have large energy density, their use can reduce energy storage equipment and containment cost by decreasing the size of the storage unit. The optimum input and output temperature of the energy storage equipment is determined by the melting point of the PCM, while the heat capacity of the TES system is determined by the PCM latent and sensible heats.

2 Objectives

The main objective of this report is to provide an assessment of molten salts and metallic alloys proposed as candidate PCMs for TES applications, particularly in solar parabolic trough electrical power plants at a temperature range from 300°C to 500°C. The physical properties most relevant for PCMs service were reviewed from the candidate selection list. Some of the PCM candidates were characterized for: chemical stability with some container materials; phase change transformation temperatures; and latent heats.

3 Methodology

3.1 Background of PCM Materials

Kenisarin (2010) published a review of high-temperature PCMs. The review considers PCMs evaluated since 1960. It includes the melting point and heat of fusion of different systems including chlorides, fluorides, hydroxides, nitrates, carbonates, vanadates, and molybdates, among others.

Williams in 2006 reported that lighter salts (containing elements with low atomic number) tend to exhibit better heat-transfer performance. A number of fluoride salt compositions were evaluated in detail (e.g., eutectic compositions of LiF-BeF_2, NaF-BeF_2, LiF-NaF-KF, and NaF-ZrF_4) for the Next Generation Nuclear Plant (NGNP) and the Nuclear Hydrogen Initiative (NHI) hydrogen-production plant. Applications in the nuclear industry are more often for heat transfer fluids rather than TES systems, but much of the required property data is the same. Oxygen-containing salts (nitrates, sulfates, and carbonates) were excluded from the evaluation because they do not possess the necessary thermochemical stability at high temperatures (over 700°C).

Williams also reported that other salts that fulfill the high temperature and chemical stability requirements were chloride salts and alkali fluoroborates (MBF_4, M = alkali element). The properties of these salts were reviewed and evaluated. Beryllium fluoride-containing salts were excluded from consideration because of the potential toxicity of beryllium compounds and their high cost. Ranking of chloride and alkali fluoroborate salts based upon corrosion characteristics was found to be inconclusive. Williams stated that improved chemistry methods were needed to produce high-purity chloride salts for corrosion studies. It has been reported that melting point and heat capacity increase in the following order: nitrates, chlorides, carbonates, and fluorides (Hoshi et al., 2005).

Knowledge of the thermal properties of a particular molten salt is important for its selection as a thermal storage material. In order to decrease the LCOE, operation of the CSP system must be matched to the operational characteristics of the TES system. For example, PCM TES can be optimized for use with a sensible HTF by using a cascade of materials with equally spaced melting points and uniform thermal properties. However, the information on the thermal properties of molten salt systems at high temperatures is currently incomplete or contradictory.

Corrosivity is a critical consideration in a TES system designed to run at high temperature for three decades. The high-temperature container materials that are able to resist the aggressive chemical behavior of the molten salts used in NGNP are basically high-temperature alloys (some stainless steels, Inconel, and Hastelloy-N), graphite, and ceramics (Williams 2006). The author reported that some important factors should be considered for molten salts as coolants for NGNP: i) corrosive behavior can occur at high temperatures (e.g., halides of Fe and Zn are usually highly corrosive); ii) heavy halide salts containing bromine and iodine usually have poor heat-transfer and high cost; and iii) mixed-halide salts with dissimilar halide anions (mixtures of chlorides, fluorides, bromides, and iodides) are considerably more complicated systems to prepare and understand.

Discrepancies have been found in the literature regarding the melting points and thermal properties associated with a particular chemical composition for molten salt systems. The identification of an accurate melting point of a PCM formulation as well as its thermal properties is key for advancing TES technologies.

To evaluate the chemical compatibility of some molten salts with certain construction and crucible materials, preliminary corrosion tests were developed. Future work will include the verification of the information predicted by the thermochemical evaluations as well as the information collected from the open literature.

3.2 PCM Studies at NREL

The candidate PCM identification was obtained using phase diagrams in which the stability region of different phases as well as the invariant reactions occurring in the system were established. An invariant reaction is a physicochemical reaction between phases that occur at a constant temperature. The reactants and products are well-differentiated phases like liquids and solids. The invariant reactions in which a liquid phase is participating are the eutectic and the peritectic reactions. The eutectic reaction occurs when a liquid phase solidifies into two solids of different compositions. Because these solids are formed simultaneously, they are a perfect intimate mixture with a particular microstructure. A peritectic reaction occurs when a liquid and a solid react during solidification to form a solid phase different than the initial solid phase. The eutectic temperature represents the minimum temperature in which the liquid phase is stable in that particular system.

Some of the phase diagrams reviewed were obtained from old databases like Phase Diagrams for Ceramists, and some were evaluated using thermochemical software called FactSage. Using this software, some diagrams were built based on the thermodynamic stability of different phases. FactSage can also report the minimum temperature at which the liquid phase is stable (eutectic temperature) and the associated chemical composition for that point (eutectic composition). All the invariant reactions that are occurring are also resolved, as well as their respective compositions and temperatures. The invariant reaction that was considered for this study was eutectic because during heating, all the solid phase will produce 100% of liquid at only one temperature.

Another important characteristic that was considered in selecting PCMs was their congruent melting point. In a congruent melting point, the solid will melt, forming a liquid with the same composition. The pure and intermediate compounds fall in this category.

There is another type of phase diagram called isomorph in which all compositions form a solid solution. Generally, when solid solutions are formed, the melting of any composition will occur in a temperature range between the solidus (beginning of melting where the first liquid forms) and the liquidus (end of melting where the last solid melts). Some isomorph systems have a unique temperature at which solidus and liquidus intercept and the composition will behave like pure components having only one melting temperature. This intercept is called congruent melting temperature in the isomorph systems, and it is of interest for this study.

Because of the complexity of storing gases, the phase change transformation of interest is the solid-liquid. This transformation should occur at only one invariant temperature in order to maximize the efficiency of the PCM when absorbing and storing the heat. For parabolic trough applications, the temperature range of interest for the PCMs is from 300°C to 500°C. The invariant temperatures considered were: i) eutectic points at which a mixture with a specific chemical composition will melt at a constant temperature, producing a liquid of the same composition as the bulk mixture; and ii) congruent melting in which a stoichiometric compound will melt at a constant temperature, producing a liquid of the same composition of the compound; under this definition are the melting points of all pure salts, metals, and materials.

To find the appropriate PCM candidates, a thermochemical evaluation was performed using different sources: Phase Diagrams for Ceramists, NIST Phase Diagrams Database, and FactSage

thermochemistry software. The molten salt systems selected include binary, ternary, and even quaternary mixtures of chlorides, fluorides, carbonates, nitrates, and bromides, among others. Metallic alloys were also considered in this study. The results from the evaluation were compared with the literature (see molten salt systems in Appendix A) (Kenisarin 2010; Forsberg, et al. 2007). Discrepancies were found not only with the chemical compositions but also with the eutectic and other invariant reaction temperatures.

Usually, single-component salts melt at high temperatures (over 700°C). The only single salts identified as PCM from 300°C to 500°C were sodium and potassium nitrates. From an industrial and practical point of view, the one-component systems are much easier to control. This consideration may make the selection of PCMs at working temperatures over 700°C (for example, for power towers) easier in some ways.

The scarcity of pure-component melting points between 300°C and 500°C indicates that multicomponent PCMs are required for the temperature range being evaluated. During the 1950s and 60s, nearly all of the binary phase and many of the ternary systems of interest for molten salts and metallic alloys were investigated. Due to the large discrepancies among the compositions and invariant reactions, the eutectic compositions and temperatures should be confirmed. For the purpose of TES, the thermal properties should also be investigated as well as their thermal stability and chemical stability with the container materials. The discrepancies could be related with the purity of the constituents, moisture (in the case of hygroscopic materials), and homogenization of mixtures, among other factors. In the present work, characterization was performed following strict protocols for handing unstable samples to obtain perfectly mixed samples. Future evaluations, including long-term chemical stability (corrosion) of construction materials in the molten salt, should be performed to obtain the final PCM list that can fulfill the requirements for advanced TES applications.

Tables 1 through 3 show the candidate PCMs selected after the thermodynamic evaluation. Binary, ternary, and quaternary systems are included. The compositions and their respective invariant temperature have been identified. The invariant reactions include: E: eutectic; P: peritectic; CM: congruent melting point; and IS: congruent melting temperature in isomorph systems. The only single-salt components identified for this temperature range were sodium nitrate and potassium nitrate. The melting points were evaluated at the laboratory and are reported as 306°C and 335°C, respectively.

Table 1. Molten salt binary systems showing the compositions and their liquidus temperatures (T_L). E: eutectic system; CM: congruent melting point; Is: Isomorph system.

Binary System		T_L, °C	Molar Fraction		Source	Notes
A	B		A	B		
KNO_3	KCl	E307.87	0.905	0.095	1	Ref 2: E320
KNO_3	K_2CO_3	E325.73	0.963	0.374	1	
LiBr	KBr	E329	0.600	0.400	1	
KNO_3	KBr	E329.84	0.924	0.076	1	
KNO_3	LiOH	E330	0.999	0.001	2	

Binary System		T_L, °C	Molar Fraction		Source	Notes
A	B		A	B		
$FeCl_2$	KCl	E350	0.390	0.610	1	
		E393	0.580	0.420		
KCl	LiCl	E352.53	0.408	0.592	1	
K_2CO_3	KOH	E365.5	0.103	0.897	1	
K_2SO_4	KOH	E376.23	0.060	0.940	1	
$FeCl_2$	NaCl	E376	0.440	0.560	1	
KCl	$MnCl_2$	E417	0.670	0.330	1	Ref 2: E420, E448
		CM494	0.500	0.500		
		E456	0.375	0.625		
LiBr	LiI	Is418	0.364	0.636	1	
KCl	$MgCl_2$	E423	0.698	0.302	1	Ref 2: E460
		E429	0.653	0.347		
		CM487	0.500	0.500		
		E473	0.416	0.584		
$MnCl_2$	NaCl	E425	0.460	0.540	1	
Li_2CO_3	LiOH	E434	0.157	0.843	1	
LiBr	LiF	E448	0.760	0.240	1	Ref 2: E453 (0.9 mol LiBr)
NaCl	$MgCl_2$	E459	0.569	0.431	1	
K_2CO_3	$MgCO_3$	E460	0.550	0.450	2	
KF	KBF_4	E460	0.255	0.745	2	
Na_2SO_4	$ZnSO_4$	E472	0.450	0.550	2	CM478 (0.5 mol Na_2SO_4)
$CaCl_2$	LiCl	E475	0.35	0.65	1	Ref 2: E496
LiCl	Li_2SO_4	E477	0.626	0.374	1	
KF	LiF	E492	0.490	0.510	1	
K_2CO_3	Li_2CO_3	E496	0.584	0.416	1	Ref 2: E491, E501
		CM503	0.500	0.500		
		E488	0.390	0.610		
Li_2CO_3	Na_2CO_3	E498	0.510	0.490	1	Ref 2: E570
LiCl	LiF	E500	0.700	0.300	1	
$CaCl_2$	NaCl	E500	0.700	0.300	2	
KVO_3	$BaTiO_3$	E500	0.980	0.020	2	Melting of KVO_3 = 520°C

1: FactSage; and, 2: Phase Diagrams for Ceramists

Table 2. Molten salt ternary systems showing the compositions and their liquidus temperatures (T_L). E: eutectic system, P: peritectic system.

Ternary System			T_L, °C	Molar Fraction			Source	Notes
A	B	C		A	B	C		
KCl	LiBr	NaBr	E276.31	0.260	0.642	0.098	1	Ref 2: E320
			P?280.26	0.299	0.597	0.104		
			P?420.71	0.420	0.137	0.443		
			P?439.61	0.594	0.056	0.350		
KBr	LiCl	NaCl	E302.64	0.327	0.491	0.182	1	Ref 2: E340°C, P354, P375
LiBr	NaBr	KBr	E308.33	0.551	0.100	0.350	1	Ref 2: E324°C, P362, P400
NaOH	NaCl	Na_2CO_3	P?320.39	0.723	0.277	0.072	1	
			P?358.85	0.678	0.322	0.093		
KCl	LiCl	Li_2SO_4	E324	0.572	0.365	0.063	2	
$MgCl_2$	KCl	NaCl	E331.31	0.343	0.657	0.251	1	Ref 2:E385, E540, P420, P430
			E331.87	0.376	0.624	0.303		
			P?339.1	0.320	0.680	0.219		
			P?357	0.288	0.712	0.183		
NaCl	KCl	$FeCl_2$	E332.55	0.330	0.335	0.335	1	
KCl	LiCl	CaF_2	E339.06	0.373	0.597	0.030	1	
$CaCl_2$	KCl	LiCl	E338.36	0.573	0.427	0.517	1	Ref 2: E340, E425
			E?429.33	0.353	0.142	0.506		
NaCl	KCl	LiCl	E344.31	0.075	0.381	0.544	1	
KF	AlF_3	ZrF_4	E380	0.540	0.062	0.398	2	
$MnCl_2$	KCl	NaCl	E380.95	0.299	0.566	0.701	1	
Na_2SO_4	K_2SO_4	$ZnSO_4$	E385	0.284	0.174	0.542	2	
Na_2CO_3	K_2CO_3	Li_2CO_3	E390.19	0.739	0.261	0.413	1	
KCl	NaCl	Li_2SO_4	E426	0.340	0.230	0.430	2	
KF	NaF	LiF	E454	0.420	0.115	0.465	2	
LiCl	NaCl	Li_2SO_4	E458	0.540	0.166	0.295	2	

1: FactSage, 2: Phase Diagrams for Ceramists

Table 3. Molten salt quaternary systems showing the compositions and their liquidus temperatures (T_L). E: eutectic temperature.

Quaternary System				T_L, °C	Molar Fraction				Source
A	B	C	D		A	B	C	D	
LiCl	KCl	$CaCl_2$	CaF_2	E330	0.561	0.424	0.715	0.715	2
KCl	NaCl	LiCl	Li_2SO_4	E428	0.113	0.155	0.535	0.198	2

2: Phase Diagrams for Ceramists

Some of the molten salt candidates that were identified in sources like Phase Diagrams for Ceramists were also found in the FactSage database, allowing for a more detailed analysis of composition and temperatures. For those salts, an evaluation of the composition that provided the lowest melting temperature of the system (eutectic point) was performed. The eutectic composition and its temperature were obtained as well as the compositions and temperatures of other invariant temperatures, like the peritectic and congruent melting points. For a particular composition, FactSage provided heat capacities for the solid and liquid phases. The heat of fusion was calculated from the solid and liquid enthalpies reported by FactSage. Table 4 shows the results from FactSage predictions.

Table 4. FactSage predictions for solid and liquid heat capacities (Cp) and heat of fusion (ΔH_m) at the liquidus temperature (T_L) for different molten salt systems.

System Components			Weight Percentage			T_L, °C	Cp, J/g.K		ΔH_m, J/g
A	B	C	A	B	C		Solid	Liquid	
$NaNO_3$			100.00			mp306	1.859	1.830	178.56
KNO_3			100.00			mp335	1.439	1.480	100.19
KNO_3	KCl		92.82	7.18		E307.87	1.156	1.177	105.63
KNO_3	K_2CO_3		65.31	34.69		E325.73	0.812	0.832	71.58
KNO_3	KBr		91.15	8.85		E329.84	1.161	1.161	100.93
$FeCl_2$	KCl		52.08	47.92		E350	0.706	0.938	133.91
KCl	LiCl		54.75	45.25		E352.53	1.009	1.279	267.96
K_2CO_3	KOH		22.05	77.95		E365.5	1.332	1.394	164.35
K_2SO_4	KOH		16.54	83.46		E376	1.329	1.408	174.09
$FeCl_2$	NaCl		63.02	36.98		E376	0.768	0.983	249.54
LiBr	KBr		52.26	47.74		E327.8	0.562	0.672	333.05
NaOH	NaCl	Na_2CO_3	59.65	24.68	15.67	P?320.39	1.649	1.835	175.17
$MgCl_2$	KCl	NaCl	42.05	39.07	18.88	E331.31	0.857	1.031	198.45
$MgCl_2$	KCl	NaCl	46.23	30.90	22.87	E331.87	0.859	1.033	207.14
NaCl	KCl	$FeCl_2$	22.24	28.80	48.96	E332.55	1.326	1.695	308.88
$CaCl_2$	KCl	LiCl	10.37	53.11	36.52	E338.36	0.950	1.200	241.24
$MgCl_2$	KCl	NaCl	39.23	44.28	16.49	P?339.1	0.863	1.037	199.67

System Components			Weight Percentage			T_L, °C	Cp, J/g.K		ΔH_m, J/g
A	B	C	A	B	C		Solid	Liquid	
$MgCl_2$	KCl	NaCl	35.35	50.84	13.81	P?357	0.870	1.032	202.70
NaOH	NaCl	Na_2CO_3	53.83	26.63	19.54	P?358.85	1.668	1.807	190.59
$MnCl_2$	KCl	NaCl	42.90	48.14	8.96	E380.95	0.752	0.946	177.27
Na_2CO_3	K_2CO_3	Li_2CO_3	34.13	35.69	30.19	E390.19	1.54 - 1.71	1.602	34.76

mp: melting point; E: eutectic; P: peritectic; ?: questionable

3.3 Characterization Procedures

Different molten salts have been identified in this study. Some of them were tested for chemical stability, melting points, and latent heat determination. The single salts were provided by Alfa-Aesar and Sigma Aldrich. The majority of the salts are in anhydrous form and have purity levels over 99%.

NREL's TES Materials Laboratory has a differential scanning calorimeter (DSC) and a thermogravimetric analysis (TGA) with differential scanning calorimetry (DSC), or TGA/DSC, from Mettler-Toledo, Inc. The TGA measures the weight changes during a controlled temperature program. DSC is based on the heat flux principle in which the heat flux of a sample and a reference measurement are compared. These instruments are employed to determine heat capacities, latent heats, transformation temperatures, and thermal/chemical stability. The laboratory also has a rheometer from TA Instruments for viscosity measurements. In-house thermal conductivity and density measurement instruments are being constructed.

The TGA instrument uses a platinum-rhodium disk as a crucible holder in which an R-type thermocouple is placed directly under the holder to guarantee that the temperature is measured very close to the sample. Besides recording the sample weight and temperature, this instrument provides a heat flow signal and thereby offers the possibility of DSC. The heat flow signal is obtained from temperature readings and calculated by multiplying the SDTA signal with the calorimetric sensitivity. The SDTA signal is the difference between the measured sample temperature and the values set in the temperature program. The temperature accuracy for the TGA/DSC is ±0.25K, and its temperature precision is ±0.15K.

DSC is a highly sensitive measuring instrument due to the sensitive ceramic sensor used to measure the difference between the heat flows of the sample and the reference. In this instrument the heat flow is measured using the sensor with its 120 gold-gold/palladium thermocouples. The calorimetric data resolution of the DSC is 0.01 μW, the temperature accuracy is ±0.20K, and its temperature precision is ±0.02K.

Before performing the DSC evaluations, the chemical stability (corrosion) of the DSC's crucible materials in the presence of the molten salt needs to be determined. Typically, the crucible materials employed are made of low-carbon 316 stainless steel (SS316L) or aluminum. The TGA/DSC can use aluminum oxide crucibles, which are more stable than SS316L or aluminum to chemical attack from such salts. When using the TGA/DSC, the thermal properties will not be as accurate as those obtained from the DSC, but it will provide a close value that will help understand the thermal behavior of that particular system.

Each formulation was prepared by drying the individual salts at 120°C for 48 hrs. The dried salts were combined at a specific ratio and the mixtures were placed in a special ceramic container and put back in the oven at 120°C to remove any water absorbed during the weighing procedure. After one hour the formulation was removed from the oven and mixed for one hour in a powder mixer. The mixing procedure was carefully controlled because the sample weight for the DSC and TGA tests are on the order of few milligrams, so a perfectly homogenized sample is essential for accurate results.

For those samples that are unstable when exposed to air (oxygen, moisture, CO_2) or have an otherwise complicated drying procedure, a handling protocol under nitrogen atmosphere is used. The weighing and placement of the powder in the mixer jar is performed inside a dry glove box under nitrogen atmosphere. The jar will be sealed under this atmosphere to avoid exposure to air during the mixing process. The mixture will be placed in a porcelain crucible and put immediately in the high-temperature furnace under nitrogen for the corrosion test. If the chemical stability of the crucible material is good, then DSC will be performed. To test the formulation in the DSC, the sample will be placed in the DSC crucible, weighed, and sealed inside the dry box. The sealed crucible can then be easily placed in the DSC instrument for analysis.

The material compatibility test for three different molten salt formulations was performed before testing them in the DSC to protect the instrument and crucibles from a possible chemical attack during the evaluations. The coupons (SS316 and aluminum) were immersed in the molten salt at 500°C for one-, three- and five-hour durations. A nitrogen atmosphere was employed in order to decrease the oxygen potential and emulate the working conditions of the DSC tests. A non-reactive porcelain crucible was employed to contain the molten salt and the coupon was tested.

For those formulations that did not attack the coupons, DSC evaluations were performed to obtain the temperatures and latent heats of each endothermic and/or exothermic reaction. Solid-solid and solid-liquid transformations were identified. The melting point, or in some cases the temperature range of melting, and their respective heat of fusion were evaluated.

To determine the solid and liquid heat capacities for the PCMs, DSC evaluations were performed following the ASTM E-1269-05 standard. This method uses a sapphire disk as a reference material. The heat capacity of the sample at a specific temperature is obtained using the known heat capacity of the sapphire and the masses of the sapphire and sample, and the heat flows through the sapphire and sample for that particular temperature. The software STARe from Mettler-Toledo was used to calculate the heat capacities.

4 Preliminary Results and Analysis

Some molten salt PCM candidates for cascaded PCMs have been evaluated. Two temperature buckets were considered: 350°C and 380°C. Three molten salt formulations were tested for chemical compatibility with two container materials, and some DSC and TGA/DSC evaluations were performed. The molten salt systems were taken from the open literature. The compositions and eutectic temperature were indicated to be in the range of 350°C and 380°C. The melting points reported by the open literature differs from the values calculated by FactSage or found in the Phase Diagrams for Ceramists database. Evaluations of these systems were performed in order to confirm the values reported in the literature. The molten salt systems evaluated were:

A. Bucket of 350°C
   1. NaCl(34.81 wt%)-KCl(32.29 wt%)-LiCl(32.90 wt%) (LUZ, 1988)

      T_m = 346°C; ΔH_m = 281 J/g

   2. KNO_3(80.69 wt%)-KBr(11.87 wt%)-KCl(7.44 wt%) (LUZ, 1988)

      T_m = 342°C; ΔH_m = 140 J/g

B. Bucket of 380°C
   3. $MgCl_2$(60 wt%)-KCl(20.4 wt%)-NaCl(19.6 wt%) (Michels and Pitz-Paal, 2007)

      T_m = 380°C; ΔH_m = 400 J/g

Formulation Number Two (KNO_3-KBr-KCl)

From FactSage and the Phase Diagrams for Ceramists database, this system does not have a ternary eutectic. In fact, the composition relies on a stability region for two phases under equilibrium: liquid and solid. These two sources predicted that this composition will melt during a temperature range with a beginning of melting (solidus temperature) and an end of melting (liquidus temperature) instead of having a constant temperature of melting, which is the case for eutectic points and congruent melting points.

This formulation was tested with a coupon of SS316 for 5.5 hrs at 500°C. The nominal composition of the salt was 80.69 wt.%KNO_3-11.87 wt.%KBr-7.44 wt.%KCl. The final composition was 80.68 wt.%KNO_3-11.87 wt.%KBr-7.45 wt.%KCl. The initial and final weights of the coupon were 1.7782 g and 1.7786 g, respectively. SS316 was chemically stable under the previous conditions. It did not show any chemical attack from the KNO_3-KBr-KCl molten salt. Another corrosion test was performed using aluminum metal immersed in this formulation. The aluminum coupon was kept at 500°C for one hour. After the test the coupon was stable and was not attacked by the molten salt.

DSC was perfomed using high-pressure stainless steel 316L (HPSS) crucibles (see plots in Appendix B). Because the expected melting point for this formulation is 342°C, it was initially evaluated from 300°C to 380°C at 10°C/min during five heating cycles (see Appendix B.a). Table 5 shows the temperature of the endothermic transformation and its associated latent heat

(ΔH_m) for each cycle. It was assumed that this transformation was the melting of the formulation (T_m). The first cycle shows a higher latent heat because it represents the melting of the powder mixture in which the stable phases are not yet formed and the melting of the individual components require more energy. Once it is melted, it is expected that the formulation becomes homogeneous and its subsequent melting will resolve its real melting point. After reaching the steady state, after the first cycle, the average melting point of this formulation is 325.58°C (σ = 1.41) and the average heat of fusion is 6.92 J/g (σ = 1.79). The expected values for the melting point and heat of fusion are 342°C and 140 J/g, respectively. The temperature of this transformation is 16°C lower than the reported melting point, and its latent heat is only 5% of the expected value. More evaluations were performed in order to understand this behavior.

Table 5. DSC results for 80.68 wt.%KNO_3-11.87 wt.%KBr-7.45 wt.%KCl from 300°C to 380°C during five heating cycles. Expected melting point, T_m = 342°C and heat of fusion, ΔH_m = 140 J/g.

Cycle	T_m, °C	ΔH_m, J/g (endothermic)
1	327.99	10.19
2	327.68	9.55
3	325.10	5.67
4	324.85	5.92
5	324.70	6.54

A second series of tests was performed from 100°C to 450°C at 10°C/min using HPSS crucibles (see Appendices B.b.i and ii). Two endothermic reactions were identified under these conditions. The first reaction occurred at about 129.06°C with a latent heat of 33.17 J/g. This reaction appears to be a solid-solid transformation. The second peak could be associated with the melting of the formulation. There are too many artifacts in the DSC plots during the heating of the sample using the stainless steel crucible. The melting of the formulation was not completely resolved under the test conditions.

The area of the second endothermic peak, which seems to be the melting of the sample, was smaller than the solid-solid transformation. This is an anomaly because the melting of any material always requires more energy. If this formulation melts in a range of temperatures, as predicted by FactSafe and the Phase Diagrams for Ceramists database, a second peak or change in slope should appear below the baseline of the DSC plot. This will represent the end of the melting or the liquidus temperature in which 100% of the liquid phase is obtained. The first peak for the melting transformation will represent the eutectic reaction or the solidus temperature in which the first liquid is obtained. In order to determine the end of the melting (liquidus temperature), a third series of tests were performed in segments from 100°C to 450°C. Artifacts were not observed under those conditions. The only transformations resolved were endothermic: solid-solid and solid-liquid.

The third series of evaluations was performed in sections. The first section was from 100°C to 180°C (see Appendices B.c.i and ii) using HPSS crucibles. As typical, the latent heat of the first cycle is higher than the other cycles due to the initial arrangement of the individual components during the first heating cycle. After this "conditioning," the system is considered to have reached

the steady state. Table 6 shows the solid-solid transformation temperatures (Ts_1-s_2) and their latent heats (ΔHs_1-s_2) for each heating cycle. The solid-solid transformation was confirmed by opening the crucible and looking the state of the sample. It was still in powder form. After reaching the steady state, the average solid-solid transformation temperature is 129.36°C (σ = 0.16) and its average latent heat is 17.64 J/g (σ = 0.40). The second section was from 180°C to 300°C. There were no transformations in this temperature range.

Four heating and cooling cycles were performed between 300°C to 450°C at 15°C/min using the aluminum crucibles to obtain a better heat flux resolution (see Appendices B.d.i, ii, iii, and iv). DSC results are shown in Table 7. The results confirm the predictions from FactSage and Phase Diagram database. This formulation, 80.68 wt.%KNO_3-11.87 wt.%KBr-7.45 wt.%KCl, is not a eutectic composition. Its melting process occured in a range of temperatures. A beginning and an end of melting/solification was obtained.

Table 6. Solid-solid transformation for 80.68 wt.%KNO_3-11.87 wt.%KBr-7.45 wt.%KCl from 100°C to 180°C during three heating cycles.

Cycle	Ts_1-s_2, °C	ΔHs_1-s_2, J/g (endothermic)
1	128.50	35.29
2	129.47	17.92
3	129.24	17.36

Table 7. Solid-liquid transformations for 80.68 wt.%KNO_3-11.87 wt.%KBr-7.45 wt.%KCl from 300°C to 450°C during four heating and cooling cycles. Average (Av.) and standard deviation (σ) are shown.

	Heating/Melting					Cooling/Solidification						Super cooling
	Solidus, °C		Liquidus °C	$\Delta T_{melt.}$ °C	ΔH_m J/g	Solidus, °C		Liquidus, °C		$\Delta T_{solid.}$ °C	$\Delta H_{sol.}$ J/g	
Cycle	Onset	Peak				Onset	Peak	Onset	Peak			ΔT, °C
1	328.5	331.82	-	-	76.67	324.12	323.02	407.84	403.37	83.72	75.10	-
2	327.06	329.75	412.63	85.57	71.88	324.42	323.25	408.54	405.97	84.12	72.73	4.09
3	326.09	328.82	412.68	86.59	76.20	324.23	323.26	408.02	405.45	83.79	79.75	4.66
4	326.58	329.28	413.66	87.08	78.80	324.57	323.29	409.06	406.40	84.49	81.63	4.60
Av.	326.58	329.28	412.99	86.41	75.89	324.41	323.21	408.37	405.30	84.03	77.30	4.45
σ	0.49	0.47	0.58	0.77	2.90	0.17	0.12	0.55	1.34	0.35	4.10	0.31

The melting process started with an average solidus temperature or beginning of melting at 326.58°C (σ = 0.49). The end of melting occurred at an average liquidus temperature of 412.99°C (σ = 0.58). The melting process occured in a temperature range of about 86.41°C (σ = 0.77). The average heat of fusion was 75.89J/g (σ = 2.90). The heat of fusion is lower than the value reported by the literature (LUZ, 1988) but is in accordance with the amount of KNO_3 (80.68 wt.%), considering that pure KNO_3 has a heat of fusion of 97.25 J/g (obtained using the same DSC instrument and same source for KNO_3 compound).

Since this formulation shows a wide melting range of 86.41°C, it is not a good PCM candidate for TES purposes. A good PCM should have a melting process that occurs in a very short temperature range with a heat of fusion higher than 100 J/g.

Formulations Number One (NaCl-KCl-LiCl) and Number Three ($MgCl_2$-KCl-NaCl)

Other chloride PCMs (NaCl-KCl-LiCl and $MgCl_2$-KCl-NaCl) were evaluated with the corrosion test in order to determine the chemical stability of SS316 and aluminum at high temperatures (500°C). Formulation number three with a nominal chemical composition of 60.00 wt.%$MgCl_2$-20.40 wt.%KCl-19.60 wt.%NaCl (380°C bucket) was prepared. The final composition was 59.98 wt.%$MgCl_2$-20.42 wt.%KCl-19.60 wt.%NaCl. The chemical stability test of this PCM showed that the SS316 coupon was corroded after exposure at 500°C for one hour. A picture of the SS316 coupon is shown in Appendix C.a. Aluminum metal was also exposed at 500°C during one hour. After that time the aluminum coupon was highly dissolved, showing an extreme corrosion/digestion attack.

The molten salt PCM number one with a nominal chemical composition of 34.81 wt.%NaCl-32.29 wt.%KCl-32.90 wt.%LiCl (350°C bucket) was prepared. The final composition was 34.81 wt.%NaCl-32.28 wt.%KCl-32.91 wt.%LiCl tested for chemical stability at 500°C for 3.5 hours with SS316. A picture of this coupon after the corrosion test is shown in Appendix C.b. This alloy was attacked by a similar way as the other chloride system. The molten salt turned a brownish color during the test, showing a strong dissolution of the iron matrix from the steel.

Due to the chemical attack of the chloride systems to SS316L and aluminum, the DSC measurements could not be performed because its crucible materials are made of these metals. Since the TGA crucibles are made of aluminum oxide (alumina) and are much more stable, TGA tests could be employed to obtain the melting point and the latent heats. In order to perform this test other preliminary evaluations must be done. The information that should be gathered includes: i) the vapor pressure of the single chlorides, and ii) a chemical stability test of the alumina with the chloride molten salt.

HSC Thermochemistry software was used to calculate the vapor pressure of different chloride and hydroxide salts. Figure 1 shows the vapor pressure from room temperature to 500°C for LiCl, $MgCl_2$, NaCl, KCl, NaOH, KOH, and LiOH. The vapor pressure of the chloride salt components of PCM numbers one and three are below 1.00×10^{-07} atm. Based on these results, TGA/DSC can be used to determine the thermal properties of these PCMs.

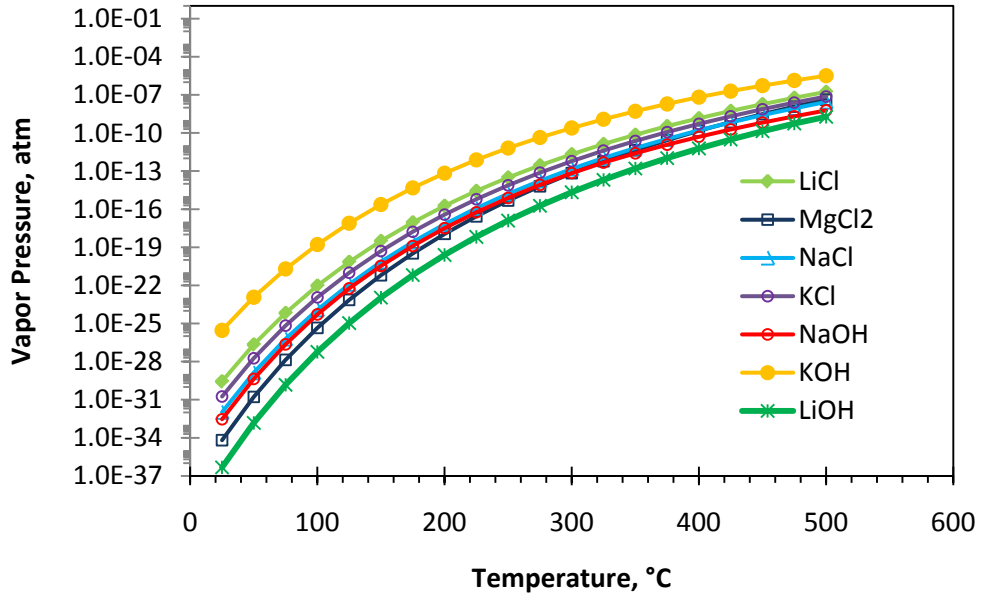

Figure 1. Vapor pressure in atm from room temperature to 500°C for LiCl, $MgCl_2$, NaCl, KCl, NaOH, KOH, and LiOH. Values were obtained from HSC Thermochemistry software. Data in Appendix D.

Before performing the evaluation of the thermal properties of these chloride systems, a water removal procedure was applied at 120°C for one hour. The weight of the sample after this procedure was considered as the initial weight for the thermal property determination. TGA/DSC were performed for both chloride PCMs from 120°C to 450°C. Three heating and cooling cycles were tested at ±10°C/min (see Appendix E). The thermal properties of PCM number one (34.81 wt.%NaCl - 32.28 wt.%KCl - 32.91 wt.%LiCl) are shown in Table 8. Plots are shown in Appendices E.a.i, ii, iii, and iv.

Table 8. TGA/DSC test for 34.81 wt.%NaCl-32.28 wt.%KCl-32.91 wt.%LiCl from 120°C to 450°C during three heating and cooling cycles. Heating and cooling rates of ±10°C /min. Expected melting point of 346°C and heat of fusion of 281 J/g.

Cycle	T_m, °C	ΔH_m, J/g	$T_{solidif}$, °C	$\Delta H_{solidif}$, J/g	$\Delta T_{supecooling}$, °C
1	351.69	164.18	350.62	124.05	1.07
2	351.66	138.55	350.18	124.35	1.48
3	350.73	125.37	349.67	122.73	1.06

Latent heats were adjusted for weight changes. Mass was lost during cycles.

The latent heat values were adjusted because there were mass losses during the cycles. The samples were not sealed because the alumina crucibles were opened to the atmosphere. They were covered by a lid having a 1-mm-diameter opening. Under the test conditions of 20 mL/min of nitrogen carrier gas, the sample was unstable, and mass losses occurred.

The average melting point of this formulation (34.81 wt.%NaCl-32.28 wt.%KCl-32.91 wt.%LiCl) was 351.36°C (σ = 0.55). The solidification occurred on average at 350.16°C (σ =

0.48). The supercooling of this formulation was on average 1.20°C (σ = 0.24). The expected melting point for this molten salt system was reported as 346°C. The difference of 5°C could be related to the purity level of the components or the preparation procedure followed. No information regarding these factors was provided by the literature.

The average heat of fusion after the steady state was 131.96 J/g (σ = 9.32) and the average heat of solidification was 123.71 J/g (σ = 0.86). The results for the latent heats are not conclusive due to mass losses. The standard deviation (σ) of the heat of fusion is too large. Further tests should be performed in order to confirm the obtained results. Characterization using other techniques should be considered later on.

The thermal properties of PCM3 (59.98 wt.%$MgCl_2$-20.42 wt.%KCl-19.60 wt.%NaCl) are shown in Table 9. TGA/DSC plots are shown in Appendices E.b.i, ii, iii, and iv. The first melting point is slightly higher because of the conditioning of the formulation. After this period, the average melting point was 381.47°C (σ = 0.79), which is fairly close to the value reported by Michels and Pitz-Paal, 2007 (380°C). The average solidification point was 383.59°C (σ = 6.45). There was no supercooling for this composition, which could be related to the formation of different compounds during the thermal cycling of the sample.

The average heat of fusion obtained (ΔH_m = 198.55 J/g (σ = 1.35)) was almost half of the expected value (400 J/g). The average heat of solidification for this PCM was 192.65 J/g (σ = 7.81). Further tests should be performed in order to corroborate the results obtained using the TGA/DSC technique.

Table 9. TGA/DSC test for 59.98 wt.%$MgCl_2$-20.42 wt.%KCl-19.60 wt.%NaCl from 120°C to 450°C during three heating and cooling cycles. Heating and cooling rates of ±10°C /min. Expected melting point of 380°C and heat of fusion of 400 J/g.

Cycle	T_m, °C	ΔH_m, J/g	$T_{solidif}$, °C	$\Delta H_{solidif}$, J/g	$\Delta T_{supecooling}$, °C
1	387.19	197.92	378.91	198.30	8.28
2	380.80	199.50	380.91	195.91	-
3	382.14	197.59	390.94	183.74	-

From the TGA/DSC plots, shown in Appendices E.b.i, ii, iii, and iv, it can be seen that during the first heating cycle an endothermic peak appeared around 238.31°C, but it disappeared during the third cycle. This reaction could be related to the removal of water chemically contained in some of the initial components like $MgCl_2$ and/or the loss of hydrogen chloride, HCl(g), due to reactions like the following: $MCl + H_2O = MO/MOH + HCl(g)\uparrow$. To evaluate this possibility, $MgCl_2$ and the formulation PCM3 were thermally treated at 300°C under air for one hour.

After this time, the treated samples were tested using X-ray diffraction (XRD). The XRD patterns are shown in Figures 1 and 2 for treated $MgCl_2$ and PCM3, respectively. After treating $MgCl_2$, the sample became extremely hygroscopic, making the handling and sample preparation extremely difficult. The results shown in Figure 2 are typical for highly moist samples. The main phase resolved was $MgCl_2.H_2O$ with a minor amount of MgO. Figure 3 shows the equilibrium phases after the heat treatment of 59.98 wt.%$MgCl_2$-20.42 wt.%KCl-19.60 wt.%NaCl. Based on the XRD pattern, part of the $MgCl_2$ was transformed into MgOHCl and K_2MgCl_4. The formation

of MgOHCl was probably due to the chemical reaction between $MgCl_2$ and H_2O, as previously discussed.

These results corroborate that the mass losses of 59.98 wt.% $MgCl_2$-20.42 wt.% KCl-19.60 wt.% NaCl are because of the decomposition of magnesium chloride to form oxides, hydroxides, and/or hydroxychlorides, with the possible liberation of HCl(g).

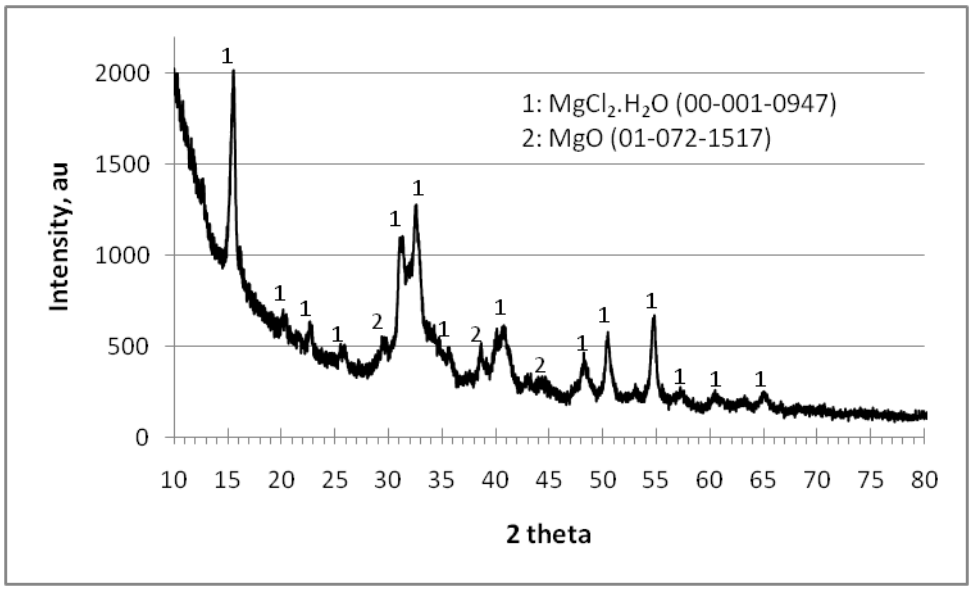

Figure 2. X-ray diffraction pattern for $MgCl_2$ treated at 300°C under air for one hour.

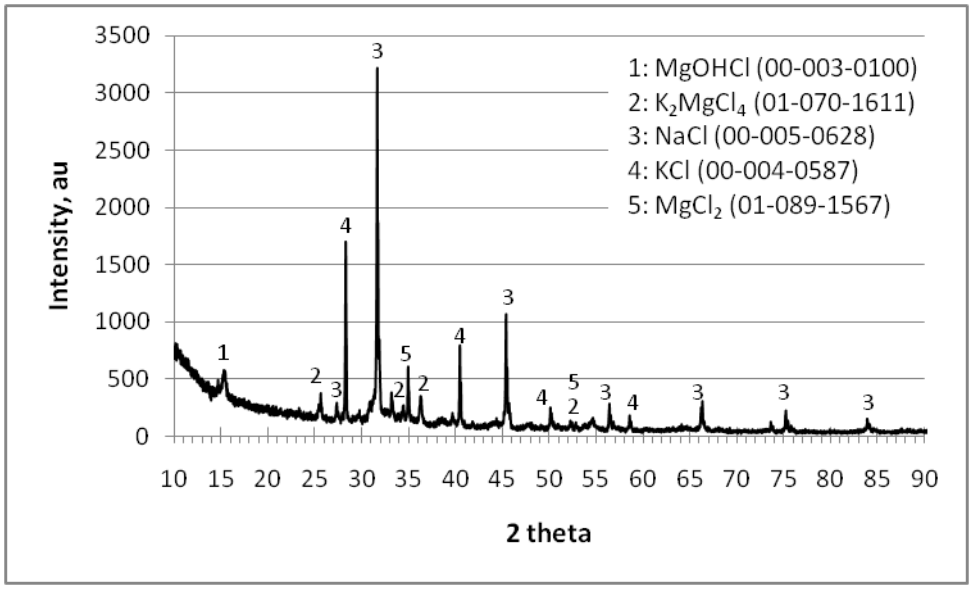

Figure 3. X-ray diffraction pattern for 59.98 wt.%$MgCl_2$-20.42 wt.%KCl-19.60 wt.%NaCl treated at 300°C under air for one hour.

5 Future Work

In order to corroborate the thermal properties predicted by FactSage, all of the binary, ternary, and quaternary systems reported in Table 4 will be tested. Metallic alloys as well as molten salt system at temperatures higher than 500°C up to 1,200°C will be considered as possible PCM candidates. Future characterization includes the determination of invariant reactions (eutectic and/or peritectic), melting/solidification temperatures, and thermal properties such as heat capacity (Cp) of solid and liquid phases, latent heats of all solid-solid and solid-liquid transformations (ΔH_t), heat conductivity, viscosity, and density, as well as the thermal and chemical stability (corrosion) at high temperatures of the crucibles and/or construction materials for the PCM containers.

Accurate values of the transformation temperatures, ΔH_t and Cp, will be obtained using DSC evaluations. For those molten salt formulations that cannot be contained in the DSC crucible materials due to chemical incompatibility, TGA/DSC will be employed to evaluate those properties. Measurements of viscosity near the melting point will be obtained by using the rheometer. Thermal conductivity and density will be also performed in the future to complete the PCMs' evaluation as possible candidates for TES applications.

The information that will be recorded for each PCM candidate is:

1. Melting point (eutectic or congruent melting points) or liquidus temperature (at which a solid phase first appears during cooling) and solidus temperature (end of solidification)
2. Working temperature range (to allow thermal and chemical stability)
3. Chemical stability with some container materials
4. Heat capacities of solid and liquid phases
5. Latent heats
6. Thermal conductivity
7. Viscosity values near the melting point
8. Liquid and solid densities
9. Cost

References

FactSage 6.2 Thermochemistry Software. Thermfact/CRCT (Montreal, Canada) and GTT-Technologies (Aachen, Germany). (2010).

Forsberg, C. W.; Peterson, P. F.; Zhao, H. (2007). "High-Temperature Liquid-Fluoride-Salt Closed-Brayton-Cycle Solar Power Towers." *Journal of Solar Energy Engineering*, 129; 141–146.

Hoshi, A.; Mills, D.; Bittar, A.; Saitoh, T. (2005). "Screening of High Melting Point Phase Change Materials (PCM) in Solar Thermal Concentrating Technology Based on CLFR." *Solar Energy*, 79; 332–339.

HSC Thermochemistry Software Version 5.11. Outotec. (2010).

Kenisarin, M. M. (2010). "High-Temperature Phase Change Materials for Thermal Energy Storage." *Renewable and Sustainable Energy Reviews*, 14(3); 955–970.

Levin, E. M.; Robbins, C. R.; McMurdie, H. F. *Phase Diagrams for Ceramists*. National Bureau of Standards, multivolume compilation from 1905 to 1989. American Ceramic Society.

LUZ Industries Israel (1988). "Thermal Storage for Medium Temperature Solar Electric Power Plants Using PCMs: A Preliminary Assessment." Phase-Change Thermal Energy Symposium, October 19-20, California.

Michels, H.; Pitz-Paal, R. (2007). "Cascaded Latent Heat Storage for Parabolic Trough Solar Power Plants." *Solar Energy*, 81; 829–837.

Williams, D. F. (2006). "Assessment of Candidate Molten Salt Coolants for the NGNP/NHI Heat-Transfer Loop." Report from Oak Ridge National Laboratory for the U.S. Department of Energy (DE-AC05-00OR22725), June 2006.

Appendices

A. Molten salt systems from review of Kenisarin 2010

Salt Composition (mol. %)	T_m, °C	ΔH_m, J/g
LiF(16.2)-42.0LiCl-17.4$LiVO_3$-11.6Li_2SO_4-11.6Li_2MoO_4	363	284 ± 7
LiF(16.2)-51.5LiCl-16.2Li_2SO_4-16.2Li_2MoO_4	402	291
*LiF(17.6-17.7)-(33.2-33.8)KF-(40.0-40.4)KCO_4-(8.6-8.6)KCl	422-426	407-412
LiF(20)-80LiOH	427	1163
LiF(25.0)-43.8$LiVO_3$-14.8Li_2SO_4-16.5Li_2MoO_4	428	260
LiF(80)-20LiOH	430	528
LiF(45.7)-1.8BaF_2-41.2KF-11.3NaF	438	332
LiF(42.5-45.5)-(41-43)KF-(10.7-11.5)NaF-(2.8-3.0)KCl	440-448	682-692
*LiF(27.1)–11.9NaF–55.1KF–5.9MgF_2	449	699
*LiF(29.2)–11.7NaF–59.1KF	454	414
LiF(46.5)–42KF–11.5–NaF	454	325
*LiF(29)–12NaF–59KF	463	442
LiF(73.6)–26.4LiCl	485	403
KF(50)–50LiCl	487	344
* LiF(33)–67KF	493	458
LiF(18.0)–53.0$LiVO_3$–29.0Li_2MoO_4	493	297
*LiCl(47.4–47.7)–(46.8–47.0)KCl–(3.2–3.4)$LiCO_3$–(2.1–2.4)LiF	340-343	375-380
LiCl(58)–42KCl	348	170
KCl(28.7)–45$MnCl_2$–26.3NaCl	350	215
KCl(45.5)–34.5$MnCl_2$–20NaCl	390	230
*LiCl(23.4–24.2)–(24.8–25.3)$LiVO_3$–(27.1–27.6)Li_2MoO_4–(17.3–17.8)Li_2SO_4–(6.1–6.2)LiF	360-363	278-284
*NaCl(22.5–26.5)–(18.5–22.5)KCl–(57.0–53.0) $MgCl_2$	385-393	405-410
KCl(21.6)–45.4$MgCl_2$–33.0NaCl	384	284
KCl(20)–50$MgCl_2$–30NaCl	396	291
KCl(22)–51$MgCl_2$–27NaCl	396	290
KCl(37.7)–37.3$MnCl_2$–25NaCl	400	235
NaCl(56)–44$MgCl_2$	430	320
*KCl(54)–46$ZnCl_2$	432	218
*KCl(61)–39$MgCl_2$	435	351
NaCl(56.2)–43.8$MgCl_2$	442	325
LiCl(58.5)–23.6Li_2SO_4–17.9Li_2MoO_4	445	327
KCl(36)–64$MnCl_2$	448	236
LiCl(49.0)–12.75Li_2SO_4–38.25$LiVO_3$	449	450
KCl(35)–65$MnCl_2$	450	237
NaCl(60)–40$MgCl_2$	450	328

A. Continuation

Salt Composition (mol. %)	T_m, °C	ΔH_m, J/g
*NaCl(48)–52$MgCl_2$	450	430
$CaCl_2$(47.6)–8.1KCl–41.3NaCl–2.9NaF	460	231
$CaCl_2$(41.6)–2.2KCl–8.8$MgCl_2$–47.4NaCl	460	245
$CaCl_2$(50)–7.25KCl–42.75NaCl	465	245
* KCl(36)–64$MgCl_2$	470	388
LiCl(69.5)–26.5LiF–4MgF_2	484	157
$CaCl_2$(50)–1.5CaF_2–48.5NaF	490	264
$CaCl_2$(52.3–55)–(45–47.2) NaCl	490-500	233-239
$CaCl_2$(52.8)–47.2NaCl	500	239
NaOH(77.2)–16.2NaCl–6.6Na_2CO_3	318	290
LiOH(80)–20LiF	427	1163
Li_2CO_3(32.1)–34.5K_2CO_3–33.4Na_2CO_3	397	276
Li_2CO_3(47)–53K_2CO_3	488-491	321-342
Li_2CO_3(44)–56Na_2CO_3	496-498	370-393
Li_2CO_3(28)–72K_2CO_3	498	263
Zn(52)–48Mg	340	180
96Zn–4Al	381	138
Al(59)–35Mg–6Zn	443	310
Mg(60)–25Cu–15Zn	452	254
Mg(52)–25Cu–23Ca	453	184
34.65Mg–65.35Al	497	285

*: weight percentage

B. Differencial Scanning Calorimeter (DSC)

a. KNO_3-KBr-KCl (Bucket 350°C)from 300°C to 380°C at 10°C/min.

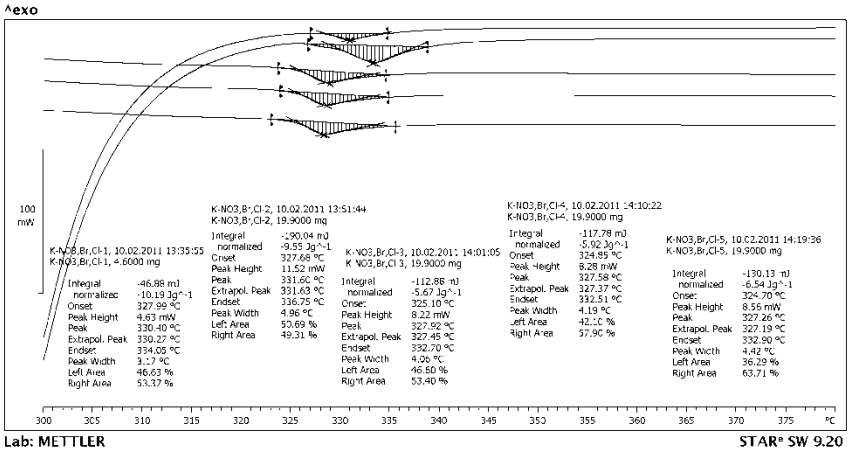

b. KNO_3-KBr-KCl from 100°C to 450°C at 10°C/min.

i. First cycle from powder materials

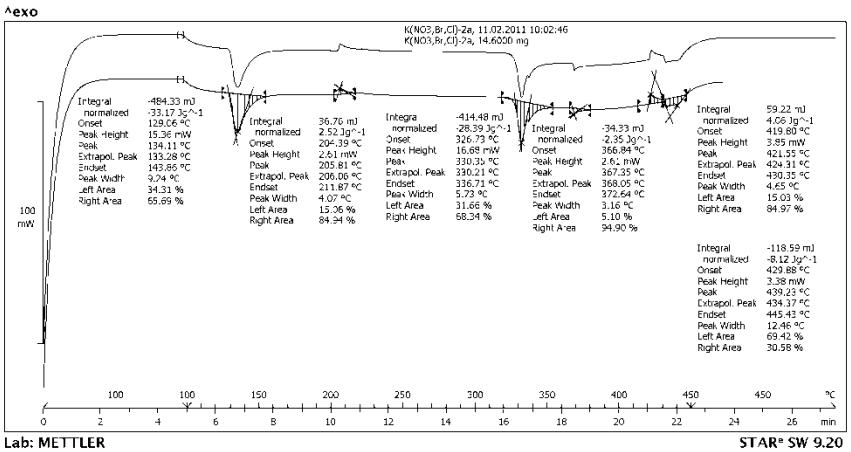

ii. Four cycles

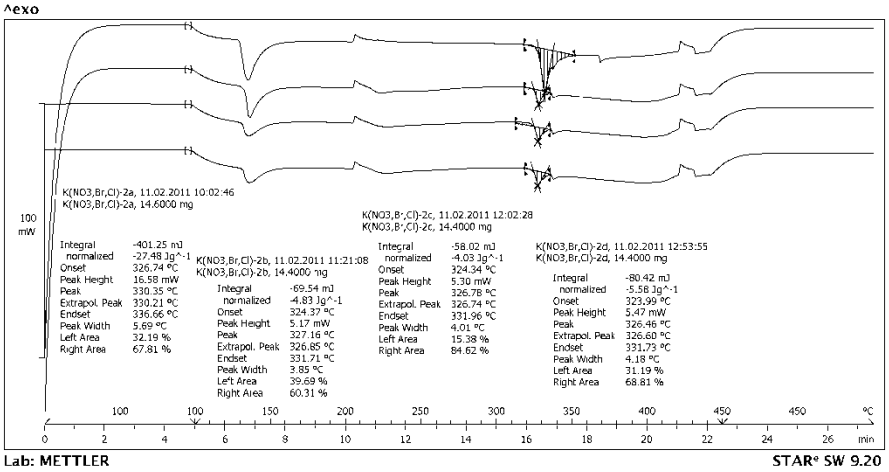

c. KNO_3-KBr-KCl from 100°C to 180°C at 10°C/min.

i. First cycle from powder materials. Solid-solid transformation.

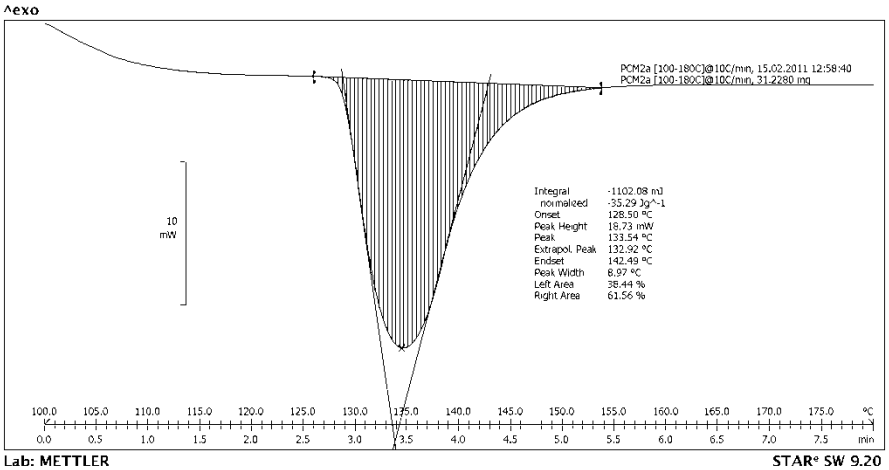

ii. Three cycles

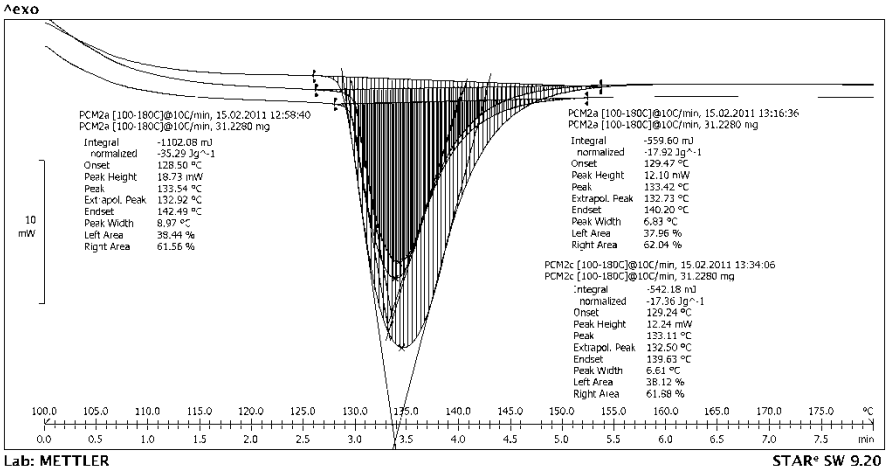

d. KNO_3-KBr-KCl formulation from 300°C to 450°C at 15°C/min using aluminum crucibles.

i. First heating/cooling cycle

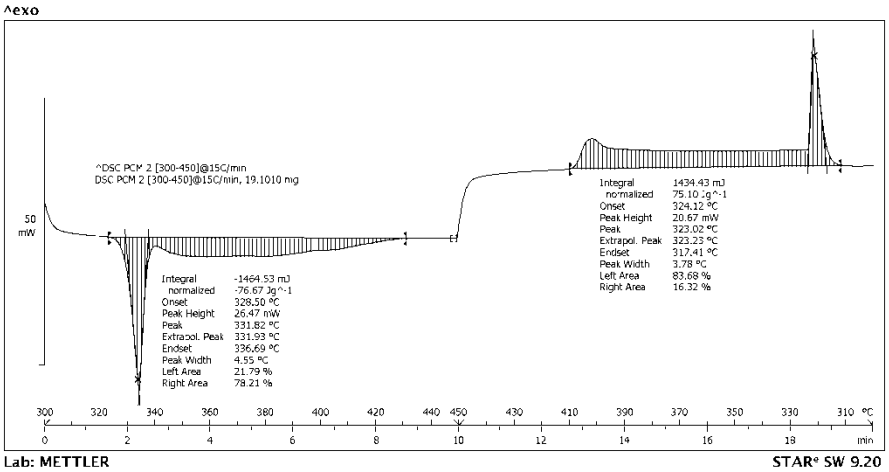

ii. Second heating/cooling cycle

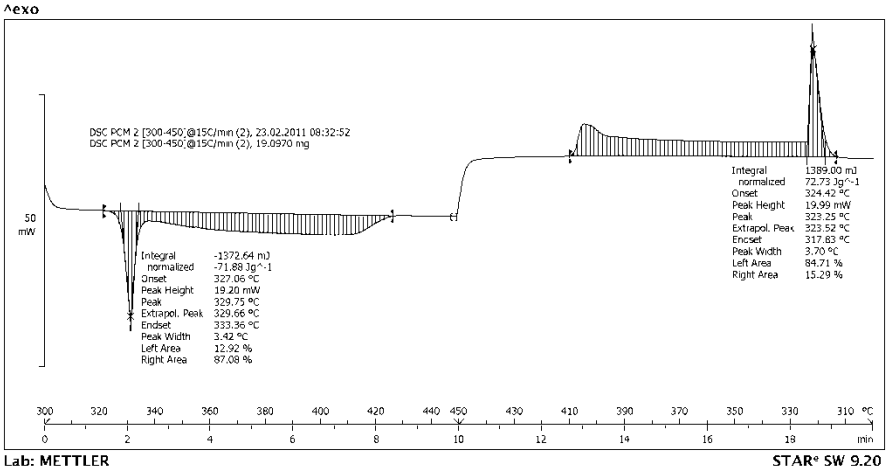

iii. Third heating/cooling cycle

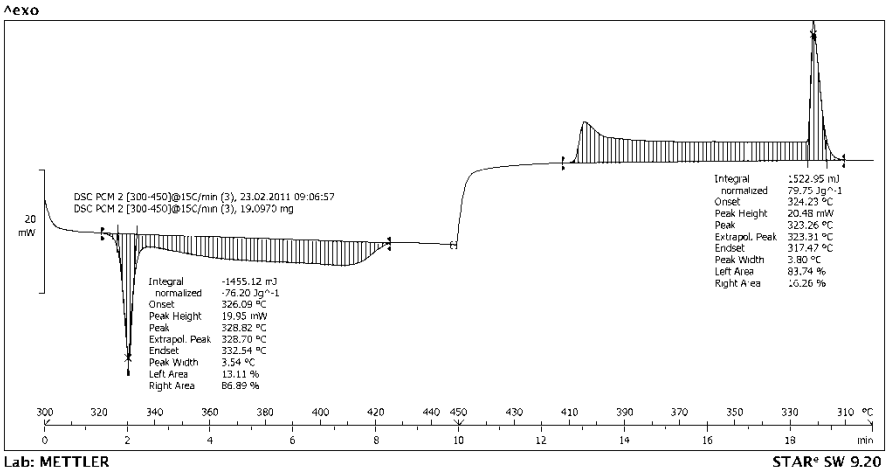

iv. Fourth heating/cooling cycle

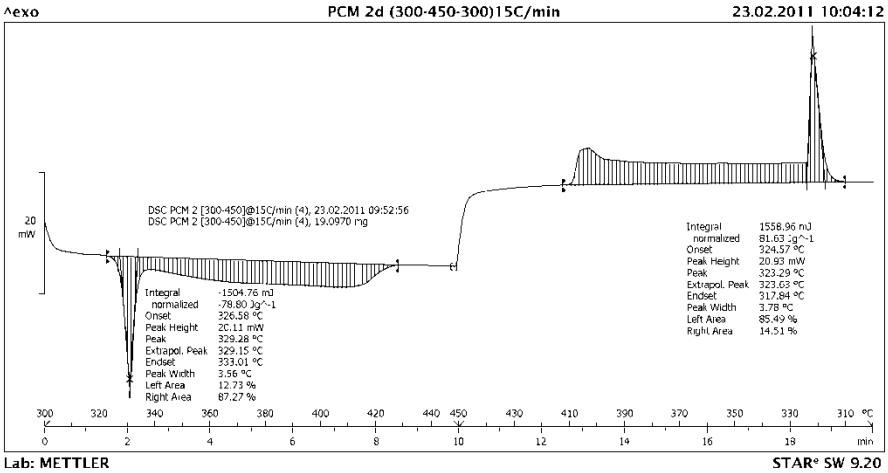

C. Chemical Stability (Corrosion) Test

a. $MgCl_2$, KCl, NaCl (Bucket 380°C). Performed at 500°C for one hour.

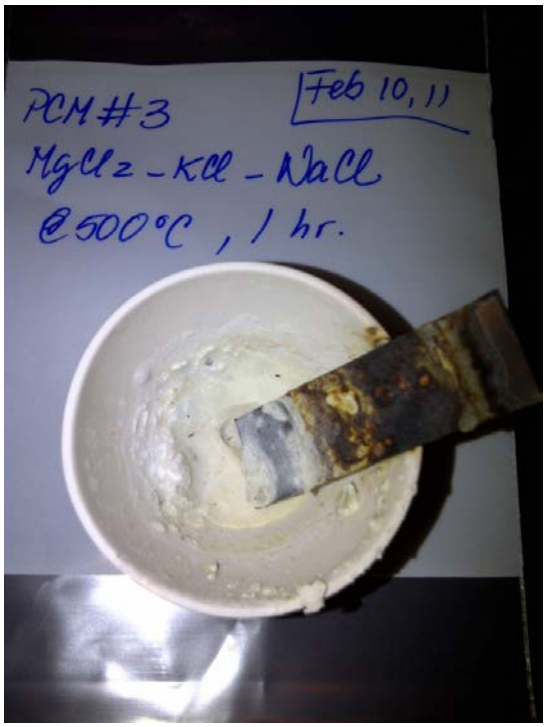

b. NaCl, KCl, LiCl (Bucket 350°C). Performed at 500°C for 3.5 hours.

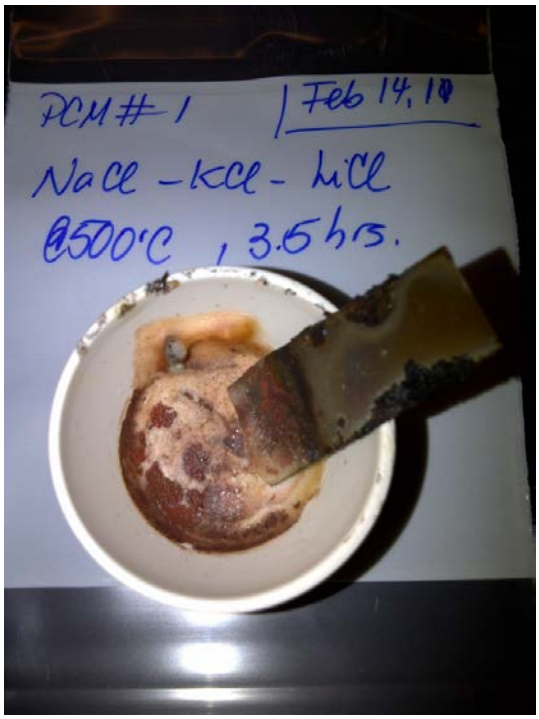

D. Values of vapor pressures of selected salts employing HSC Thermochemistry software.

	LiCl=LiCl(g)	$MgCl_2 = MgCl_2(g)$	NaCl=NaCl(g)	KCl=KCl(g)	NaOH=NaOH(g)	KOH=KOH(g)	LiOH=LiOH(g)
T, °C	P_v,atm	P_v,atm	P_v,atm	P_v,atm	P_v,atm	P_v,atm	P_v,atm
25	2.76328E-30	6.42648E-35	1.02846E-32	1.79208E-31	2.85832E-33	2.89198E-26	4.6826E-37
50	2.21977E-27	1.65673E-31	1.32312E-29	1.82614E-28	4.33324E-30	1.17051E-23	1.4924E-33
75	6.75499E-25	1.36858E-28	6.0268E-27	6.81176E-26	2.27516E-27	1.97368E-21	1.48897E-30
100	9.46931E-23	4.5553E-26	1.19814E-24	1.13889E-23	5.12117E-25	1.65393E-19	5.86887E-28
125	7.07897E-21	7.25252E-24	1.21583E-22	9.93188E-22	5.7984E-23	7.86017E-18	1.08798E-25
150	3.1558E-19	6.29614E-22	7.09761E-21	5.07186E-20	3.41356E-21	2.34303E-16	1.08383E-23
175	9.15005E-18	3.2996E-20	2.61539E-19	1.65925E-18	1.25924E-19	4.73726E-15	6.4353E-22
200	1.84764E-16	1.13107E-18	6.54531E-18	3.73272E-17	3.15362E-18	6.90974E-14	2.47147E-20
225	2.74424E-15	2.704E-17	1.17945E-16	6.11064E-16	5.67944E-17	7.6379E-13	6.55424E-19
250	3.13349E-14	4.74814E-16	1.60441E-15	7.62015E-15	7.70163E-16	6.5569E-12	1.26551E-17
275	2.85176E-13	6.38914E-15	1.71239E-14	7.51433E-14	8.17239E-15	4.3921E-11	1.85779E-16
300	2.13117E-12	6.8226E-14	1.48042E-13	6.04315E-13	6.92557E-14	2.47595E-10	2.14912E-15
325	1.34064E-11	5.95237E-13	1.06459E-12	4.06661E-12	4.61047E-13	1.20068E-09	2.01843E-14
350	7.24832E-11	4.34784E-12	6.51106E-12	2.33967E-11	2.51262E-12	5.10171E-09	1.57813E-13
375	3.42793E-10	2.71439E-11	3.45119E-11	1.17203E-10	1.19396E-11	1.92907E-08	1.04921E-12
400	1.43946E-09	1.47408E-10	1.61095E-10	5.19168E-10	5.02453E-11	6.57747E-08	6.03977E-12
425	5.43639E-09	7.06899E-10	6.71343E-10	2.06076E-09	1.89765E-10	1.96757E-07	3.05743E-11
450	1.86707E-08	3.03261E-09	2.52744E-09	7.41404E-09	6.50612E-10	5.36821E-07	1.37935E-10
475	5.88718E-08	1.177E-08	8.68423E-09	2.44166E-08	2.04511E-09	1.36323E-06	5.55658E-10
500	1.71855E-07	4.1733E-08	2.74762E-08	7.42428E-08	5.94479E-09	3.24525E-06	1.84464E-09

E. Thermogravimetric Analysis with DSC (TGA/DSC)

a. NaCl - KCl - LiCl formulation from 120°C to 450°C at ±10°C/min using aluminum oxide crucibles.

i. Three heating/cooling cycles

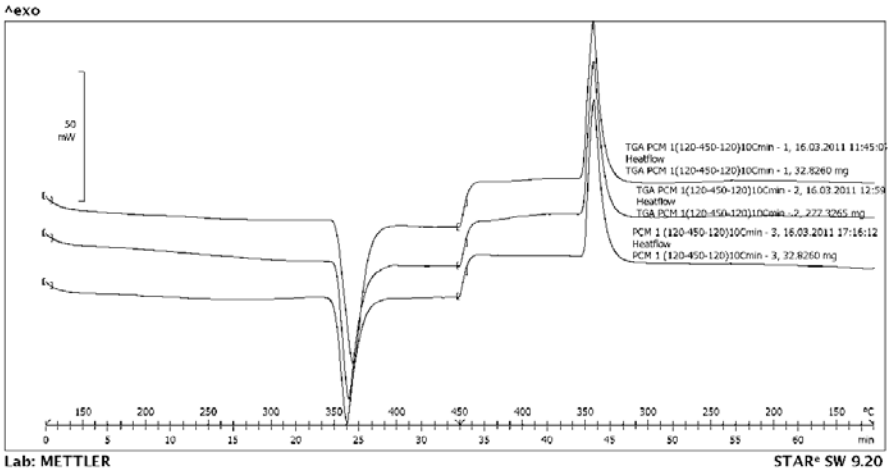

ii. First heating/cooling cycle

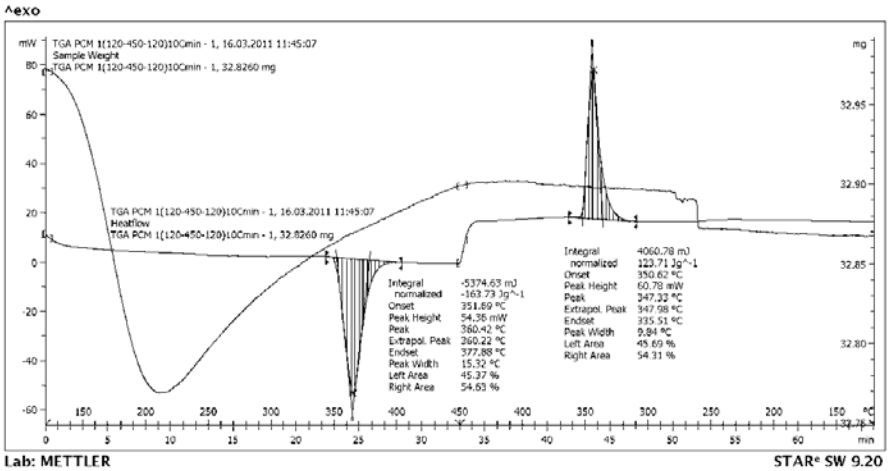

iii. Second heating/cooling cycle. Sample weight must be corrected at 32.4815 mg.

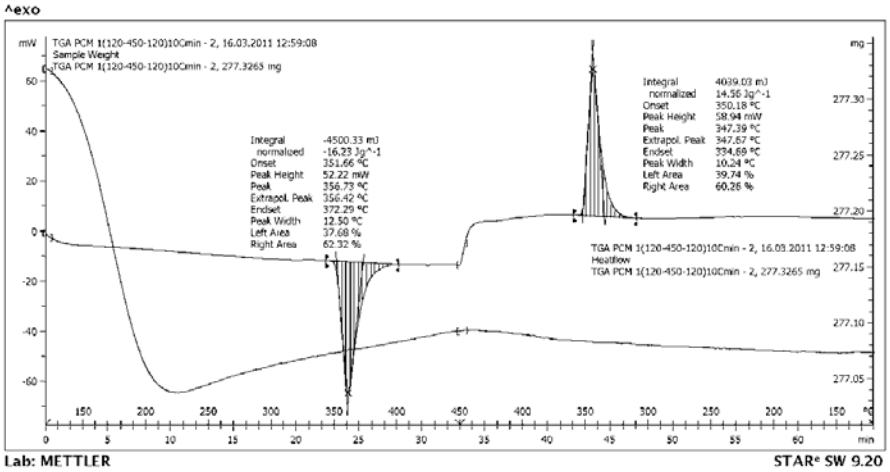

iv. Third heating/cooling cycle

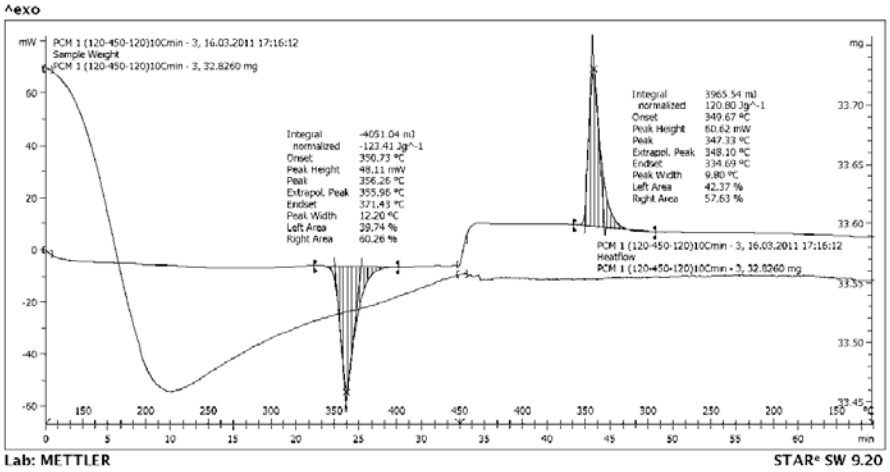

b. $MgCl_2$-KCl-NaCl formulation from 120°C to 450°C at ±10°C/min using aluminum oxide crucibles.

i. Three heating/cooling cycles

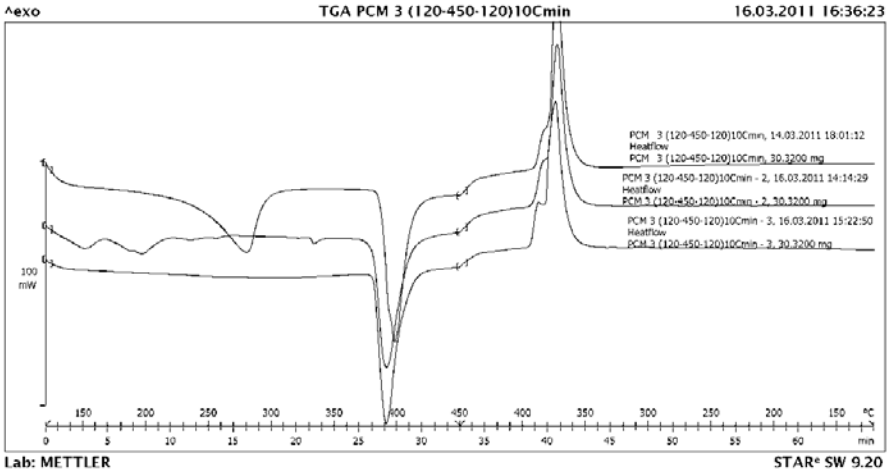

ii. First heating/cooling cycle

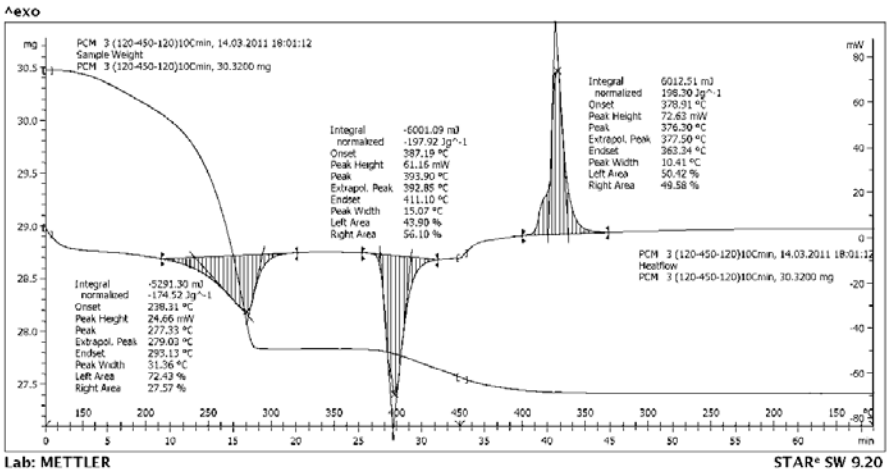

iii. Second heating/cooling cycle

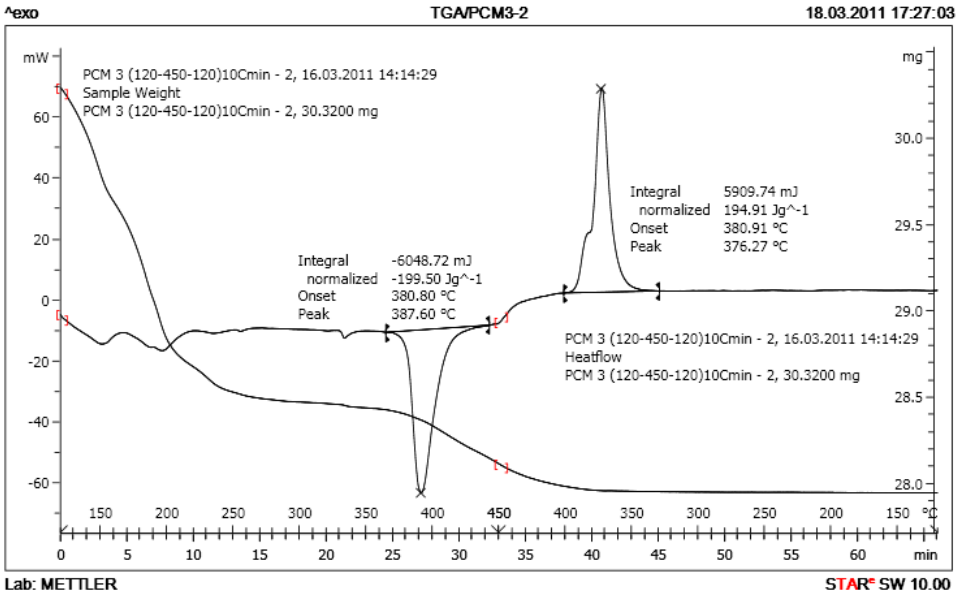

iv. Third heating/cooling cycle